FACE RECOGNITION BASED ON EXTENDED SEPARABLE LATTICE 2-D HMMS

Keisuke Kumaki, Yoshihiko Nankaku, and Keiichi Tokuda

Nagoya Institute of Technology, Nagoya, Japan

ABSTRACT

This paper proposes an extension of separable lattice 2-D hidden Markov models (SL-HMMs) for dealing with image rotation and local deformation. It is important to reduce the effect of geometrical variations in image recognition, e.g., location, size, and rotation. SL-HMMs are one of the most efficient structures to accomplish invariance to size and location variations. However, since SL-HMMs only have one state sequence in each direction, they cannot deal with rotation or local deformation. The proposed models have state sequences corresponding to all rows and columns of an input image, and the complicated state alignments can represent rotation and local deformation. The effectiveness of the proposed models was demonstrated in face recognition experiments.

Index Terms— face recognition, hidden Markov models, separable lattice 2-D HMMs, variational EM algorithm,

1. INTRODUCTION

Statistical approaches have successfully been applied to many image recognition applications. However, if images contain geometric variations such as size, location, and rotation, the recognition rate rapidly decreases. Therefore, many image recognition systems require techniques of heuristic normalization in pre-processing. It is necessary to develop a technique for each task to use such normalization techniques, because heuristic techniques usually use task dependent information. Moreover, techniques of heuristics normalization do not take classifiers into account. It is natural to use the same criterion to train both classifiers and normalization.

Hidden Markov model (HMM)-based techniques have been proposed as approaches to geometric variations. The geometric matching between input images and model parameters is represented by discrete hidden variables and the normalization process is included in the calculation of probabilities. However, the extension of HMMs to multi-dimensions generally leads to an exponential increase in the amount of computation for the training algorithm. Pseudo 2-D HMMs (or embedded HMMs) have been proposed [1], [2] and applied to many image applications to reduce computational complexity while retaining excellent properties that can model multi-dimensional data. A pseudo 2-D HMM has the states of a superior HMM horizontally, called super-states, and each super-state has a vertically one-dimensional HMM instead of a probability density function. However, the state alignments of vertically consecutive observation lines are calculated independently and this hypothesis does not always hold true in practice.

On the other hand, a more restricted structure, separable lattice 2-D HMMs (SL-HMMs) have been proposed [3]. SL-HMMs have a composite structure of multiple hidden state sequences that interact to model the observation on a lattice. SL-HMMs make it possible to model invariance to the size and location of an object. However, SL-HMMs cannot deal with rotation and local deformation. Although an extension of SL-HMMs to rotational variations has been proposed [4], it still cannot deal with more complex local deformation. We propose extended separable lattice 2-D HMMs (ExSL-HMMs), which have state sequences corresponding to all rows and columns of an input image, to deal with both rotation and local deformation. The proposed models can deal with rotation and local deformation through complicated state alignments due to increasing state alignments. We also derived a training algorithm based on the variational expectation maximization (EM) algorithm. We evaluated the effectiveness of the proposed model in face recognition experiments.

The rest of the paper is organized as follows. We briefly explain SL-HMMs in Section 2 and define ExSL-HMMs in Section 3. Section 4 presents the training algorithm we derived for the proposed models. Section 5 describes face recognition experiments we carried out on the XM2VTS database and finally we conclude the paper in Section 6.

2. SEPARABLE LATTICE 2-D HMMS

Separable lattice 2-D HMMs are defined for modeling 2-D data. The observations of 2-D data are assumed to be given on a 2-D lattice:

$$\boldsymbol{O} = \{\boldsymbol{O_t} \mid \boldsymbol{t} = (t^{(1)}, t^{(2)}) \in \boldsymbol{T}\}, \tag{1}$$

where $\boldsymbol{t}$ denotes the coordinates of the lattice in 2-D space $\boldsymbol{T}$ and $t^{(m)} = 1, \ldots, T^{(m)}$ is the coordinate of the m-th dimension. Observation $\boldsymbol{O_t}$ is emitted from the state indicated by hidden variable $\boldsymbol{S_t} \in \boldsymbol{K}$. Hidden variables $\boldsymbol{S_t} \in \boldsymbol{K}$ can take one of $K = K^{(1)}K^{(2)}$ states, which are assumed to be arranged on 2-D state lattice $\boldsymbol{K} = \{1, \ldots, K\}$. In other words, a set of hidden variables $\{\boldsymbol{S_t} \mid \boldsymbol{t} \in \boldsymbol{T}\}$ represents a segmentation of observations into K states, and each state corresponds to a segmented region in which the observation vectors are assumed to be generated from the same local deformation. Since observation $\boldsymbol{O_t}$ is only dependent on state $\boldsymbol{S_t}$ as in ordinary HMMs, the dependencies of hidden variables determine the properties and modeling ability of 2-D HMMs.

To reduce the number of possible state sequences, we constrain the hidden variables to be composed of two Markov chains:

$$\boldsymbol{S} = \{\boldsymbol{S}^{(1)}, \boldsymbol{S}^{(2)}\} \tag{2}$$

$$\boldsymbol{S}^{(m)} = \{S_1^{(m)}, \ldots, S_{t^{(m)}}^{(m)}, \ldots, S_{T^{(m)}}^{(m)}\}, \tag{3}$$

where $\boldsymbol{S}^{(m)}$ is the Markov chain along with the m-th coordinate and $S_{t^{(m)}}^{(m)} \in \{1, \ldots, K^{(m)}\}$. The composite structure of hidden variables in SL-HMMs is defined as the product of hidden state sequences: $\boldsymbol{S_t} = (S_{t^{(1)}}^{(1)}, S_{t^{(2)}}^{(2)})$. This means that the segmented regions of observations are constrained to rectangles, which allows an observation lattice to be elastic both vertically and horizontally.

The joint probability of observation vectors $\boldsymbol{O}$ and hidden vari-

ables $\boldsymbol{S}$ can be written as:

$$
\begin{aligned}
& P(\boldsymbol{O}, \boldsymbol{S} \mid \Lambda) \\
&= P(\boldsymbol{O} \mid \boldsymbol{S}, \Lambda) \prod_{m=1,2} P(\boldsymbol{S}^{(m)} \mid \Lambda) \\
&= \prod_{\boldsymbol{t}} P(\boldsymbol{O_t} \mid \boldsymbol{S_t}, \Lambda) \times \\
&\quad \prod_{m=1,2} \Big[P(S_1^{(m)} \mid \Lambda) \prod_{t^{(m)}=2}^{T^{(m)}} P(S_{t^{(m)}}^{(m)} \mid S_{t^{(m)}-1}^{(m)}, \Lambda) \Big], \quad (4)
\end{aligned}
$$

where Λ is a set of model parameters.

3. EXTENDED SEPARABLE LATTICE 2-D HMMS

Separable lattice 2-D HMMs make it possible to model invariance to variations in the size and location of an object. However, SL-HMMs cannot deal with rotation or local deformation. The reason for this is that the segmented regions of observations are constrained to rectangles because SL-HMMs only have one state sequence in each direction. We propose ExSL-HMMs to deal with rotation and local deformation, which have state sequences corresponding to all rows and columns of an input image. The hidden variables representing state sequences are defined as:

$$
\begin{aligned}
\boldsymbol{S} &= \{\boldsymbol{S}^{(1)}, \boldsymbol{S}^{(2)}\} && (5) \\
\boldsymbol{S}^{(1)} &= \{\boldsymbol{S}_1^{(1)}, \ldots, \boldsymbol{S}_{t^{(2)}}^{(1)}, \ldots, \boldsymbol{S}_{T^{(2)}}^{(1)}\} && (6) \\
\boldsymbol{S}^{(2)} &= \{\boldsymbol{S}_1^{(2)}, \ldots, \boldsymbol{S}_{t^{(1)}}^{(2)}, \ldots, \boldsymbol{S}_{T^{(1)}}^{(2)}\} && (7) \\
\boldsymbol{S}_{t^{(2)}}^{(1)} &= \{S_{1,t^{(2)}}^{(1)}, \ldots, S_{t^{(1)},t^{(2)}}^{(1)}, \ldots, S_{T^{(1)},T^{(2)}}^{(1)}\} && (8) \\
\boldsymbol{S}_{t^{(1)}}^{(2)} &= \{S_{t^{(1)},1}^{(2)}, \ldots, S_{t^{(1)},t^{(2)}}^{(2)}, \ldots, S_{T^{(1)},T^{(2)}}^{(2)}\} && (9) \\
S_{t^{(1)},t^{(2)}}^{(m)} &\in \{1, 2, \ldots, K^{(m)}\} && (10)
\end{aligned}
$$

The composite structure of hidden variables in ExSL-HMMs is defined as the product of hidden sequences: $\boldsymbol{S_t} = (S_{t^{(1)},t^{(2)}}^{(1)}, S_{t^{(1)},t^{(2)}}^{(2)})$. The joint probability of observation vectors $\boldsymbol{O}$ and hidden variables $\boldsymbol{S}$ can be written as:

$$
\begin{aligned}
& P(\boldsymbol{O}, \boldsymbol{S} \mid \Lambda) \\
&= P(\boldsymbol{O} \mid \boldsymbol{S}, \Lambda) P(\boldsymbol{S} \mid \Lambda) \\
&= \prod_{\boldsymbol{t}} P(\boldsymbol{O_t} \mid \boldsymbol{S_t}, \Lambda) \\
&\quad \times \prod_{t^{(2)}=1}^{T^{(2)}} \Big[P(S_{1,t^{(2)}}^{(1)} \mid \Lambda) \prod_{t^{(1)}=2}^{T^{(1)}} P(S_{t^{(1)},t^{(2)}}^{(1)} \mid S_{t^{(1)}-1,t^{(2)}}^{(1)}, \Lambda) \Big] \\
&\quad \times \prod_{t^{(1)}=1}^{T^{(1)}} \Big[P(S_{t^{(1)},1}^{(2)} \mid \Lambda) \prod_{t^{(2)}=2}^{T^{(2)}} P(S_{t^{(1)},t^{(2)}}^{(2)} \mid S_{t^{(1)},t^{(2)}-1}^{(2)}, \Lambda) \Big] \\
& \qquad\qquad\qquad\qquad\qquad\qquad\qquad\qquad\qquad\qquad (11)
\end{aligned}
$$

Figure 1 shows a graphical representation of an ExSL-HMM. The model parameters of an ExSL-HMM are summarized as:

1) $\boldsymbol{\Pi}^{(m)} = \{\pi_i^{(m)} \mid 1 \le i \le K^{(m)}\}$: the initial state probability distribution, where $\pi_i^{(1)} = P(S_{1,t^{(2)}}^{(1)} = i)$ is the probability of state i at $t^{(1)} = 1$ in the 1-th state sequence and $\pi_i^{(2)} = P(S_{t^{(1)},1}^{(2)} = i)$ is the probability of state i at $t^{(2)} = 1$ in the 2-th state sequence.

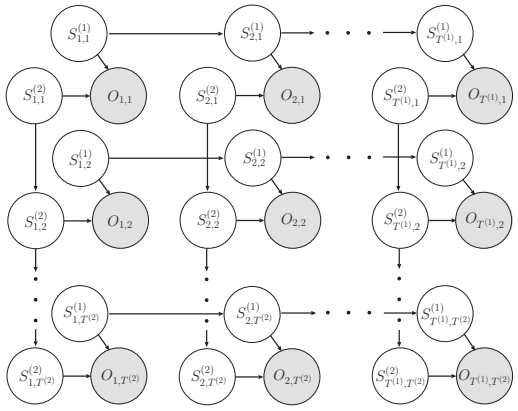

Fig. 1. Extended separable lattice HMM

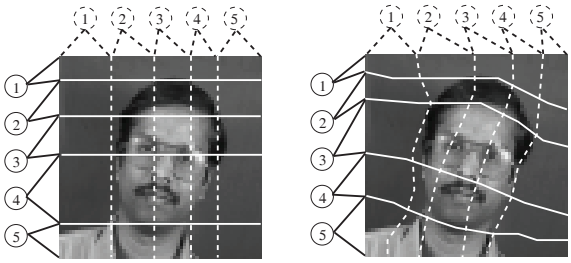

(a) SL-HMM (b) ExSL-HMM

Fig. 2. Examples of state alignments

2) $\boldsymbol{A}^{(m)} = \{a_{ij}^{(m)} \mid 1 \le i, j \le K^{(m)}\}$: the transition probability matrix, where $a_{ij}^{(1)} = P(S_{t^{(1)},t^{(2)}}^{(1)} = j \mid S_{t^{(1)}-1,t^{(2)}}^{(1)} = i)$ is the transition probability from i to state j in the 1-th state sequence and $a_{ij}^{(2)} = P(S_{t^{(1)},t^{(2)}}^{(1)} = j \mid S_{t^{(1)},t^{(2)}-1}^{(2)} = i)$ is the transition probability from i to state j in the 2-th state sequence.

3) $\boldsymbol{B} = \{b_{\boldsymbol{k}}(\boldsymbol{O_t}) \mid \boldsymbol{k} \in \boldsymbol{K}\}$: the output probability distributions, where $b_{\boldsymbol{k}}(\boldsymbol{O_t}) = P(\boldsymbol{O_t} \mid \boldsymbol{S_t} = \boldsymbol{k}, \Lambda)$ is the probability of observation vector $\boldsymbol{O_t}$ at state $\boldsymbol{k}$ on state lattice $\boldsymbol{K}$ and is assumed to be a single Gaussian distribution: $P(\boldsymbol{O_t} \mid \boldsymbol{S_t} = \boldsymbol{k}, \Lambda) = \mathcal{N}(\boldsymbol{O_t}; \mu_{\boldsymbol{k}}, \Sigma_{\boldsymbol{k}})$ where $\mu_{\boldsymbol{k}}$ and $\Sigma_{\boldsymbol{k}}$ correspond to the mean vector and the covariance matrix.

Using shorthand notation, ExSL-HMMs are defined as:

$$
\Lambda = \{\Lambda^{(1)}, \Lambda^{(2)}, \boldsymbol{B}\},\ \Lambda^{(m)} = \{\Pi^{(m)}, \boldsymbol{A}^{(m)}\} \qquad (12)
$$

Note that although ExSL-HMMs have a larger number of hidden variables and can represent more complicated state alignments than SL-HMMs, ExSL-HMMs have exactly the same set of model parameters as SL-HMMs.

Figure 2 shows examples of state alignments to a rotated face of SL-HMM and ExSL-HMM. The SL-HMM (Figure 2(a)) cannot appropriately segment the rotated face. However, the ExSL-HMM (Figure 2(b)) can obtain appropriate state alignments to the image. Furthermore, ExSL-HMMs are not only expected to deal with rotation but also local deformation.

4. TRAINING ALGORITHM FOR EXSL-HMMS

The parameters of ExSL-HMMs can be estimated using the EM algorithm, which is an iterative procedure for approximating the maximum likelihood (ML) estimate. This procedure maximizes the expectation of complete data log-likelihood, the so-called $\mathcal{Q}$-function:

$$\mathcal{Q}(\Lambda, \Lambda') = \sum_{\boldsymbol{S}} P(\boldsymbol{S} \mid \boldsymbol{O}, \Lambda) \ln P(\boldsymbol{S}, \boldsymbol{O} \mid \Lambda') \tag{13}$$

The re-estimation formula in the M-step can easily be derived by maximizing the $\mathcal{Q}$-function with respect to model parameters Λ. However, calculating posterior distribution $P(\boldsymbol{S} \mid \boldsymbol{O}, \Lambda)$ in the E-step is computationally intractable due to the combination of hidden variables. We applied the variational EM algorithm [5] to train the ExSL-HMMs to derive a feasible algorithm.

The variational method approximates the posterior distribution over the hidden variables by using a tractable distribution. Any distribution $Q(\boldsymbol{S})$ over the hidden variables defines a lower bound on the log likelihood:

$$\begin{aligned} \ln P(\boldsymbol{O} \mid \Lambda) &= \ln \sum_{\boldsymbol{S}} Q(\boldsymbol{S}) \frac{P(\boldsymbol{S}, \boldsymbol{O} \mid \Lambda)}{Q(\boldsymbol{S})} \\ &\geq \sum_{\boldsymbol{S}} Q(\boldsymbol{S}) \ln \frac{P(\boldsymbol{S}, \boldsymbol{O} \mid \Lambda)}{Q(\boldsymbol{S})} \\ &= \mathcal{F}(Q, \Lambda), \end{aligned} \tag{14}$$

where Jensen's inequality has been applied. The difference between $\ln P(\boldsymbol{O} \mid \Lambda)$ and $\mathcal{F}$ is given by the Kullback-Leibler (KL) divergence between $Q(\boldsymbol{S})$ and posterior distribution $P(\boldsymbol{S} \mid \boldsymbol{O}, \Lambda)$. Therefore, maximizing lower bound $\mathcal{F}$ with respect to $Q(\boldsymbol{S})$ is equivalent to minimizing KL divergence, and provides an approximate distribution for posterior distribution $P(\boldsymbol{S} \mid \boldsymbol{O}, \Lambda)$. To yield a tractable algorithm, it is necessary to consider a more restricted structure for $Q(\boldsymbol{S})$ distributions. We can consider a constrained family of variational distributions for the proposed models by assuming that $Q(\boldsymbol{S})$ factorizes over subsets $Q(\boldsymbol{S}^{(1)}_{t^{(2)}})$ and $Q(\boldsymbol{S}^{(2)}_{t^{(1)}})$, so that:

$$Q(\boldsymbol{S}^{(1)}, \boldsymbol{S}^{(2)}) = \prod_{t^{(2)}} Q(\boldsymbol{S}^{(1)}_{t^{(2)}}) \prod_{t^{(1)}} Q(\boldsymbol{S}^{(2)}_{t^{(1)}}) \tag{15}$$

where $\sum_{\boldsymbol{S}^{(1)}_{t^{(2)}}} Q(\boldsymbol{S}^{(1)}_{t^{(2)}}) = 1$ and $\sum_{\boldsymbol{S}^{(2)}_{t^{(1)}}} Q(\boldsymbol{S}^{(2)}_{t^{(1)}}) = 1$. The optimal distributions of the subsets are obtained by maximizing $\mathcal{F}$ independently while keeping the other distributions fixed:

$$\begin{aligned} Q(\boldsymbol{S}^{(1)}_{t^{(2)}}) &\propto P(\boldsymbol{S}^{(1)}_{t^{(2)}} \mid \Lambda) \\ &\times \prod_{t^{(1)}} \exp\Big[\sum_{\boldsymbol{S}^{(2)}_{t^{(1)}, t^{(2)}}} Q(\boldsymbol{S}^{(2)}_{t^{(1)}, t^{(2)}}) \ln P(\boldsymbol{O}_{\boldsymbol{t}} \mid S_{\boldsymbol{t}}, \Lambda) \Big] \end{aligned} \tag{16}$$

$$\begin{aligned} Q(\boldsymbol{S}^{(2)}_{t^{(1)}}) &\propto P(\boldsymbol{S}^{(2)}_{t^{(1)}} \mid \Lambda) \\ &\times \prod_{t^{(2)}} \exp\Big[\sum_{\boldsymbol{S}^{(1)}_{t^{(1)}, t^{(2)}}} Q(\boldsymbol{S}^{(1)}_{t^{(1)}, t^{(2)}}) \ln P(\boldsymbol{O}_{\boldsymbol{t}} \mid S_{\boldsymbol{t}}, \Lambda) \Big] \end{aligned} \tag{17}$$

The E-step consists of the updates of $Q(\boldsymbol{S}^{(1)}_{t^{(2)}})$ and $Q(\boldsymbol{S}^{(2)}_{t^{(1)}})$, which interact through the expectations. The distributions $Q(\boldsymbol{S}^{(1)}_{t^{(2)}})$ and $Q(\boldsymbol{S}^{(2)}_{t^{(1)}})$ have the same structure as the posterior of standard HMMs by inspection; the forward-backward algorithm can be used to compute a new set of expectations. Therefore, the complexity of E-step with the variational approximation becomes $O(K^{(1)}T^{(1)}K^{(2)}T^{(2)} + \{K^{(1)}\}^2T^{(1)}T^{(2)} + \{K^{(2)}\}^2T^{(1)}T^{(2)})$. Although this is higher than the complexity of SL-HMMs: $O(K^{(1)}T^{(1)}K^{(2)}T^{(2)} + \{K^{(1)}\}^2T^{(1)} + \{K^{(2)}\}^2T^{(2)})$, it is still computationally feasible.

5. EXPERIMENTS

We conducted face recognition experiments on the XM2VTS database [6] to demonstrate the modeling ability of ExSL-HMMs. We prepared eight images of 100 subjects; six images were used for training and two for testing. Face images on a gray scale of 64×64 pixels were extracted from the original images. Two datasets were prepared with this process:

- "dataset 1": rotation normalized data.
- "dataset 2": data with rotational variations. All images were transformed with randomly rotational angles generated within $-10 \sim 10$ degrees from a uniform distribution.

The data were modeled using 2-D HMMs with 8×8, 16×16, 24×24, 32×32, and 40×40 states and single Gaussian distributions. The transition probabilities for each state sequence were assumed to have a left-to-right and top-to-bottom no skip topology. We used two kinds of feature vectors, i.e., the pixel values and 2-D discrete cosine transform (2-D DCT) coefficients of images. We calculated the 2-D DCT coefficients with the following method. Input images were scanned using a window (12×12) that shifted by 1 pixel from left-to-right and top-to-bottom, and the 2-D DCT coefficients were calculated from each scanned block. Only 4×4 coefficients of the lowest frequencies in the 2-D DCT domain were used as feature vectors. The conditions for calculating the 2-D DCT coefficients were determined through preliminary experiments.

Four models were constructed to compare the accuracy of recognition: embedded HMMs that had horizontally ("Emb-H-HMMs") and vertically ("Emb-V-HMMs") embedded states, "SL-HMMs", and "ExSL-HMMs". Figures 3 and 4 show the recognition rates on "dataset 1" and "dataset 2" with the pixel values as feature vectors. Emb-H-HMMs, Emb-V-HMMs, and ExSL-HMMs obtained worse results than SL-HMMs. This is because Emb-H-HMMs, Emb-V-HMMs, and ExSL-HMMs could obtain more complicated state alignments than SL-HMMs. This caused the state alignments to over-fit. Figures 5 and 6 show the recognition rates with the 2-D DCT coefficients as feature vectors on "dataset 1" and "dataset 2". Emb-H-HMMs, Emb-V-HMMs and ExSL-HMMs had better recognition rates than SL-HMMs in both datasets, and ExSL-HMMs particularly had the best recognition rates. This is because 2-D DCT coefficients included shape information on all block regions. This prevented the state alignments from over-fitting. ExSL-HMMs were more effective with "dataset 2" (with rotation variations) than with "dataset 1" (with no rotation variations). This is because ExSL-HMMs could deal with rotational variations.

Figure 7 shows examples of the visualized state alignments on "dataset 2". Emb-H-HMM and Emb-V-HMM have been omitted. The first row represents the visualized mean vectors and the first column represent those of the test dataset. The visualized alignments indicate matching between the models and test data and these are represented by the mean values of the states corresponding to observations of the testing data. It is clear that SL-HMMs cannot deal with rotation variations in either pixel values or 2-D DCT coefficients. Conversely, ExSL-HMMs can be fitted to the rotated image

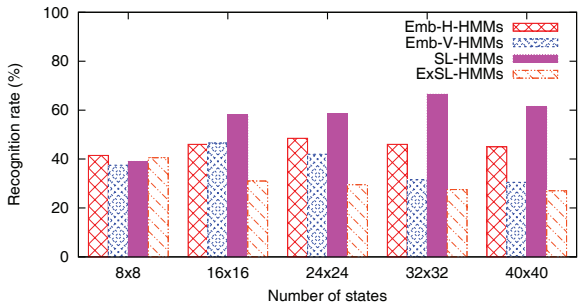

Fig. 3. Recognition rates on "dataset 1" (pixel values)

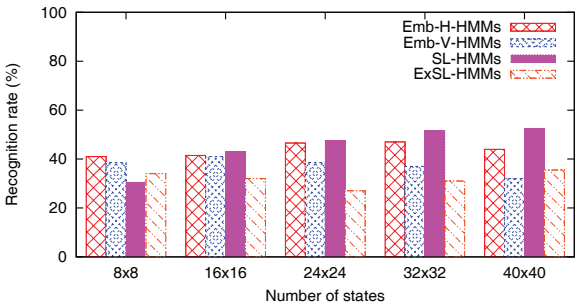

Fig. 4. Recognition rates on "dataset 2" (pixel values)

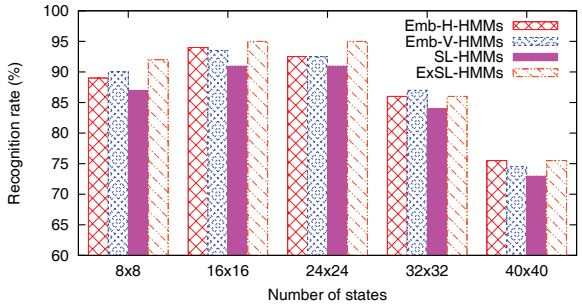

Fig. 5. Recognition rates on "dataset 1"(2-D DCT coefficients)

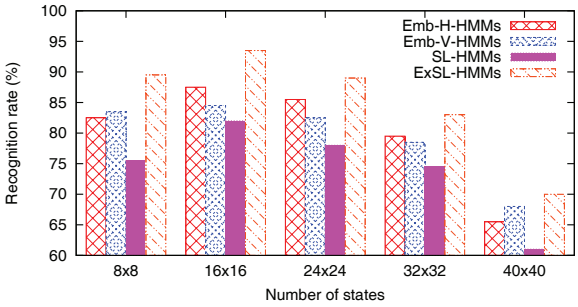

Fig. 6. Recognition rates on "dataset 2"(2-D DCT coefficients)

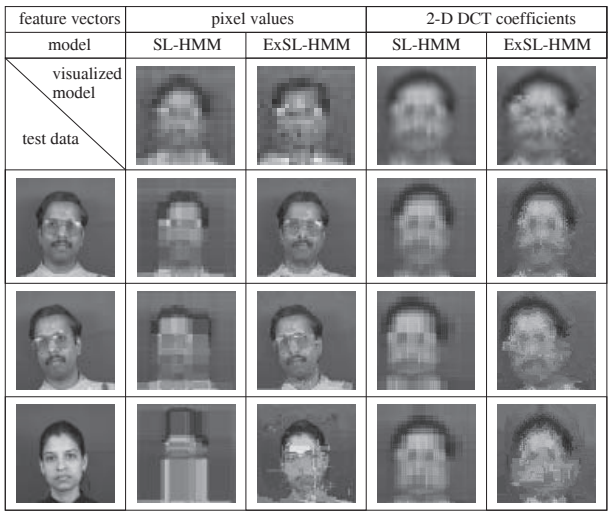

Fig. 7. Examples of visualized state alignments on "dataset 2". Top and middle test data are correct class data on visualized models, and bottom data are incorrect class data.

due to the flexible structure of the model. However, ExSL-HMMs over-fitted the test data with pixel values because they were fitted to incorrect class data. However, over-fitting was prevented with 2D-DCT coefficients by using the shape information in the blocks, and this led to higher recognition-rates.

6. CONCLUSION

We proposed ExSL-HMMs and presented a training algorithm based on variational approximation. Face recognition experiments were performed on the XM2VTS database with 2-D DCT coefficients. The proposed models achieved better results than embedded HMMs and standard SL-HMMs. We intended to do experiments using data with different variations, rotation-invariant features, and state duration modeling in future work.

7. ACKNOWLEDGEMENTS

This work was partially supported by the Hori Sciences & Arts Foundation and the Artificial Intelligence Research Promotion Foundation.

8. REFERENCES

[1] S. Kuo, and O. E. Agazzi, "Keyword Spotting in Poorly Printed Documents Using Pseudo 2-D Hidden Markov Models," IEEE Trans. Pattern Analysis and Machine Intelligence, vol.16, no.8, pp.842-848, 1994.

[2] A. Nefian, and M. H. Hayes III, "Maximum Likelihood Training of Embedded HMM for Face Detection and Recognition," Proc. ICIP, vol.1, pp.33-36, 2000.

[3] D. Kurata, Y. Nankaku, K. Tokuda, T. Kitamura, and Z. Ghahramani, "Face Recognition Based on Separable Lattice HMMs," IEEE International Conference on Acoustics, Speech, and Signal Processing, pp.737-740, 2006.

[4] A. Tamamori, Y. Nankaku, and K. Tokuda, "An Extension of Separable Lattice 2-D HMMs for Rotational Data Variations," IEEE International Conference on Acoustics, Speech, and Signal Processing, pp.2206-2209, 2010.

[5] M. I. Jordan, Z. Ghahramani, T. S. Jaakkola and L. K. Saul, "An Introduction to Variational Methods for Graphical Models," Machine Learning, vol.37, pp.183-233, 1999.

[6] K. Messer, J. Mates, J. Kitter, J. Luettin, and G. Maitre, "XM2VTSDB: The Extended M2VTS Database," Audio and Video-Based Biometric Person Authentication, pp.72-77, 1999.